

Effect of the Structure of Anodic TiO₂ Nanotube Arrays on Its Photoelectrocatalytic Activity

Jidong Shi¹, Qun Qian², Hongyi Jiang², Haibo Li², Shengdong Wang³,
Fang Wei² & Daolun Feng^{2,*}

¹ College of Merchant Marine, Shanghai Maritime University, Shanghai, 201306, P.R. China;

² College of Ocean Science and Engineering, Shanghai Maritime University, Shanghai, 201306, P.R. China;

³ Shanghai Environmental Health Engineering Design Institute CO., LTD, Shanghai, 200232, P.R. China;

*E-mail: fengdaolun@aliyun.com

Received: 28 July 2019 / Accepted: 23 October 2019 / Published: 30 November 2019

Anodic TiO₂ nanotube arrays (TNTs) exhibit excellent photoelectrocatalytic activities. However, the influence of TNTs structure on the photoelectrocatalytic activity has not yet been explored systematically. In this study, TNTs were prepared through anodization of Ti foils in electrolytic solution followed by annealing at 350 °C. The morphologies and microstructures of the as-prepared TNTs were characterized by scanning electron microscopy and X-ray diffraction. The photoelectrocatalytic activity of the as-prepared TNTs was tested through the degradation of methyl orange dye. The photoelectrocatalytic activity of TNTs increases with its length. It only takes 28 min for 2.90 μm long TNTs to reach 98% degradation percentage, in comparison with that of 36min for 4.16 μm long TNTs and 40 min for 7.72μm long TNTs. Better integrity and smoothness of TNTs presents better photoelectrocatalytic activity. E.g.: TNTs annealed at 350 °C for 1h presents better integrity and only take 28 min to obtain 98% degradation percentage, in comparison with that of 32 min for TNTs annealed at 350 °C for 3h. The crystal structure of TNTs with preferred orientation shows better photoelectrocatalytic activity than that with random orientation, which only takes 24 min to reach 98% degradation percentage, in comparison with that of 36 min for random orientated TNTs. Consequently, the photoelectrocatalytic activity of TNTs is highly related with the structure of TNTs.

Keywords: Anodic TiO₂ nanotubes; nanotube structure; Photoelectrocatalytic activity

1. INTRODUCTION

TiO₂ nanotube arrays (TNTs) are applicable to many fields due to their unique characteristics, such as light confinement properties and charge transport [1-4]. In addition, their structures can reduce the resistance of charge carrier (electron-hole pairs) compared to the traditional TiO₂ nano-materials.

Hence, TNTs are used as photoelectrocatalysts for pollutant removal in waste water from industry [5-11], as well as air purification under ultraviolet light [12-13]. The application of potential bias voltage during photoelectrocatalysis can suppresses recombination of the photo-generated charge carriers by promoting the separation between photo-generated electrons and holes, leading to improved photocatalytic activity [14-16].

TNTs fabricated by anodization in various electrolytes presents excellent photoelectrocatalytic (PEC) activity [17], and were most extensively researched [18-20]. PEC activity of anodic TNTs is highly related to the one-dimensional transportation of photo-generated charge-carrier, hence the structure of anodic TNTs strongly influence its PEC activity [21-23]. Nevertheless, to the best of our knowledge, no studies have focused on the impacts of TNTs structure on its PEC activity systematically [24-25].

In this study, TNTs were fabricated by anodization on Ti substrates, and the influence of nanotube length, integrity and crystallographic preferred orientation of anodized TNTs on PEC activity [26-27] were investigated. The results indicated that the PEC activity of TNTs is highly related to its structure.

2. EXPERIMENTAL AND METHODS

2.1 Materials preparation

Ti foil (purity 99.99%, length*width*thickness=30 mm*25 mm*0.3mm) was provided by Beijing Zhongnuo technology company. A two-electrode configuration was used to carry out the anodization process on Ti foil, in which a stainless steel plate was employed as the cathode. The anodization was performed in 1500 mL organic electrolyte solution composed of ethylene glycol, 0.3wt.% NH_4F and 5%vol deionized water under 30 V at room temperature (22 °C) respectively. The distance between the anode and cathode was fixed at 2 cm, and magnetic stirring was maintained during the anodization process. A Zahner electrochemical workstation (Germany, Zennium) is used as the power source, and to record the current profiles during anodization process.

2.2 Fabrication of TiO_2 nanotube array and its Characterization

TNTs is prepared by electro-chemical ways to fabricate [28] in a two-electrode electro-chemical cell. First a high purity Ti foil (0.3mm thick) cleaned with acetone and deionized for 15min, separately. Secondly, the pure Ti foil was electrochemical reacted for 1h at 30 V at room temperature (22 °C) . Using the Ti foil as anode and a stainless steel plate was employed as the cathode. The electrolyte was 1500 mL organic electrolyte solution composed of ethylene glycol, 0.3wt.% NH_4F and 5%vol deionized water respectively. Finally, the as-prepared anodic TNTs were annealed in a muffle furnace (Shanghai Jinghong Laboratory Instrument Co., Ltd. SXL-1002). The annealing temperature was firstly ramped up at rate of 1 °C/min, and subsequently maintained at 350 °C for 1~ 3 h. After annealing, the samples were cooled to room temperature under air atmosphere. The as-prepared anodic TNTs were characterized by X-ray diffraction(XRD, Philip PW 1050-3710 diffract meter with $\text{Cu K}\alpha$ irradiation) and scanning electron microscopy (SEM, Hitachi SU8220) at Shanghai Institute of Ceramics of Chinese Academy of Sciences.

2.3 Electrocatalytic, photocatalytic and photoelectrocatalytic degradation of MO dye.

EC degradation: MO dye solution was prepared by dissolving 10 mg/L MO dye in 3.5 wt.% NaCl electrolyte solution. A custom-made reactor (a working, counter and reference electrodes) was used for electrocatalysis degradation experiments. The reactor holds about 150 mL of solution at a level where the anodized Ti foil was submerged just below the anodization area that is approximately 6.25 cm². 0.4 V bias voltage was used to conduct EC degradation of MO dye solution.

PC degradation: The degradation of MO dye solution in a batch-type reactor by TNTs with same lengths was conducted at the same vessels, with a volume of 150 mL of solution. TNTs with a geometric area of about 6.25 cm² were put in the reactor vessel. Pt foil with a geometric area of about 6.25 cm². 365nm wavelength irradiation was provided by Phoseon Technology (Firefly FF200, USA). The anode was kept at a 6 cm distance from the light source, luminescence intensity on TNTs surface was determined to be ~41.64 mW/cm² by Thorlabs (GmbH, S302C) light power sensor.

PEC degradation: A three-electrode system was employed, in which the anodized Ti foil with surface area of ca. 6.25 cm² was used as the working electrode. Pt foil (25*25*0.2mm) with surface area of ca. 6.25 cm² was the counter electrode, and saturated calomel electrode was applied as the reference electrode. Digital orbital shaker (WIGGENS Labortechnik GmbH, WS-100D, Germany) was utilized for shaking of MO dye solution. The distance between the working electrode and light source was 6 cm, and luminous intensity was set at ~41.64 mW/cm². For each PEC experiment, the cell was filled with 150 mL electrolyte solution.

The concentration of MO dye in solution was analyzed using a spectrometer (T6, Beijing puxi general instrument Co. Ltd) by measuring intensity in peak absorbance at 464 nm. All experiments were conducted at room temperature.

3. RESULT AND DISCUSSION

3.1 Photoelectrocatalytic activity of TiO₂ nanotube toward MO dye degradation

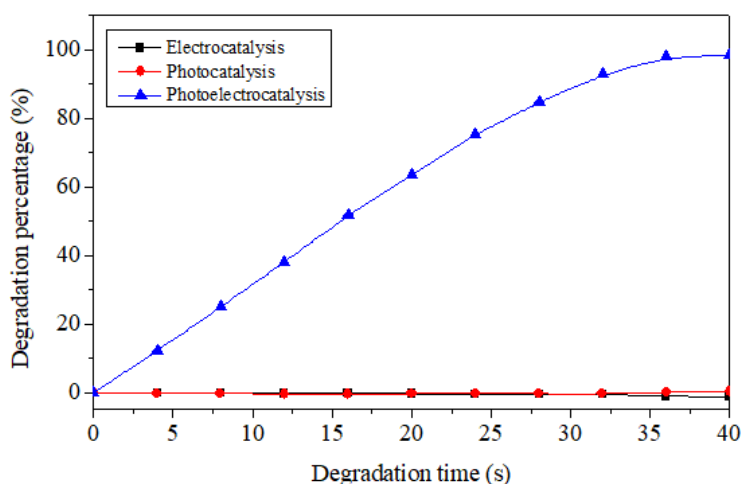


Figure 1. Electrocatalytic, photocatalytic and photoelectrocatalytic degradation performance of TNTs. Anodiation time: 60 min.

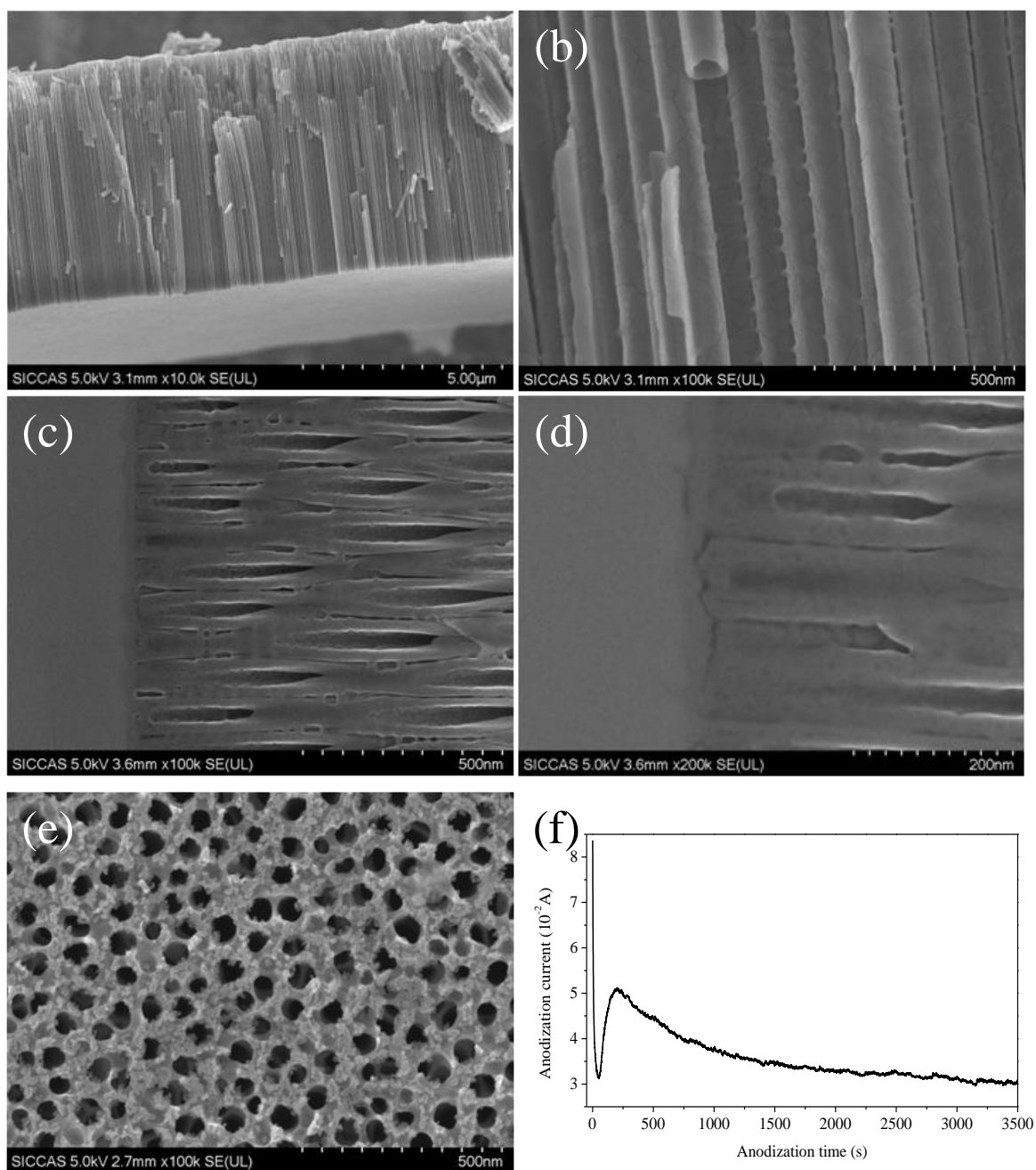


Figure 2. Cross-sectional SEM images of TNTs; (a, b) shows the side view of TNTs; (c, d) shows the details of the TNTs bottom.; (e) shows the top view of TNTs; (f) The current-time curve of TNTs fabricated by anodization. Anodization time: 60 min.

Figure 1 shows changes in degradation percentage of TNTs towards the degradation of MO dye through three ways: electrocatalysis (EC), photocatalysis (PC) [29] and photoelectrocatalysis (PEC) [30-31]. PEC shows 97% degradation after 40 min treatment. In comparison, the processes carried out without UV-vis irradiation (EC) and without current (PC) show negligible changes in MO dye concentration. The results indicated that electrical-enhanced photocatalysis can have excellent degradation activity.

Anodized TNTs were characterized by SEM and the results are depicted in Figure 2. Figure 2a and 2b show that TNTs are uniformly formed in an orderly fashion. After annealing noble cracks appears on TNTs (Figure 2c and 2d), which may have negative impact on PEC activity of TNTs. Figure 2f depicts the current-time curve of nanotubes formation. The Ti foil current shows a downward trend with a sharp drop during the initial stage related to oxide formation followed by a slow upward process representing pore erosion, and finally slow downward current indicative of nanotube formation.

3.2 Effects of TiO_2 nanotubes lengths on PEC activity

The impact of nanotube length of TNTs on its PEC activity is investigated [32-33], and the results are presented on Figure 3. In this study, 0.4V applied bias was utilized[34-35]. The PEC activity of TNTs increases with its length. It only takes 28 min for 2.90 μm long TNTs to reach 98% degradation percentage, in comparison with that of 36min for 4.16 μm long TNTs and 40 min for 7.72 μm long TNTs. on the other hand, the photocurrent response of TNTs with different nanotube length during PEC process is presented in Figure 4. Similarly, the photo-current of TNTs increases with its length. E.g.: the photo-current for 2.90 μm long TNTs reaches 8.1mA after 40 min degradation. In contrast, that for 7.72 μm long TNTs only has 5.5 mA.

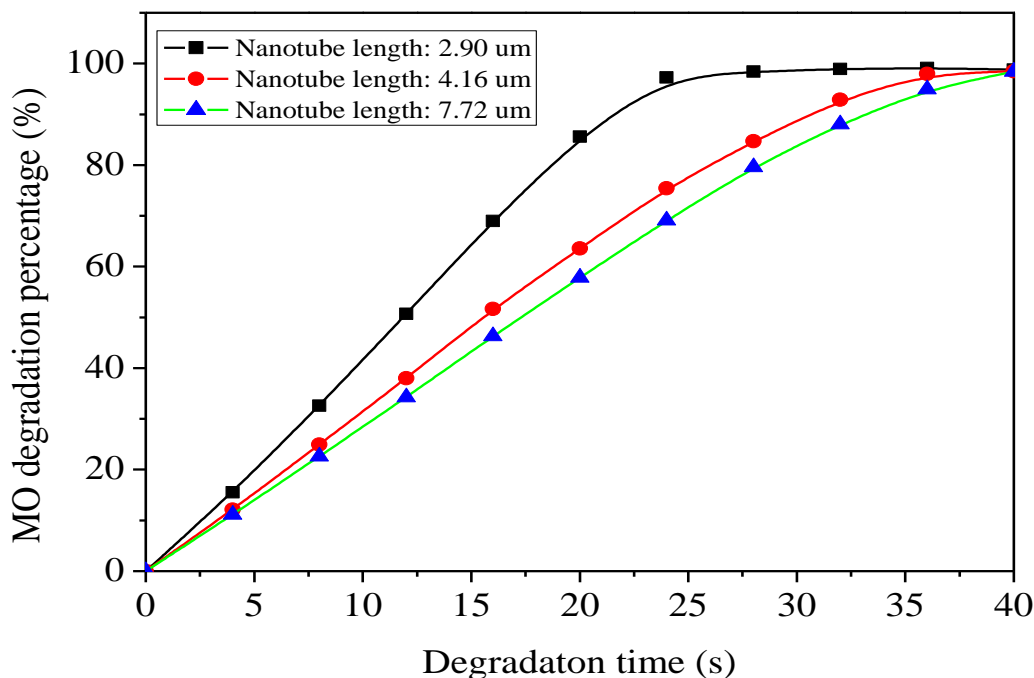


Figure 3. Photoelectrocatalytic degradation performance of TNTs with different nanotube length. All experiments were conducted at +0.4 V applied bias.

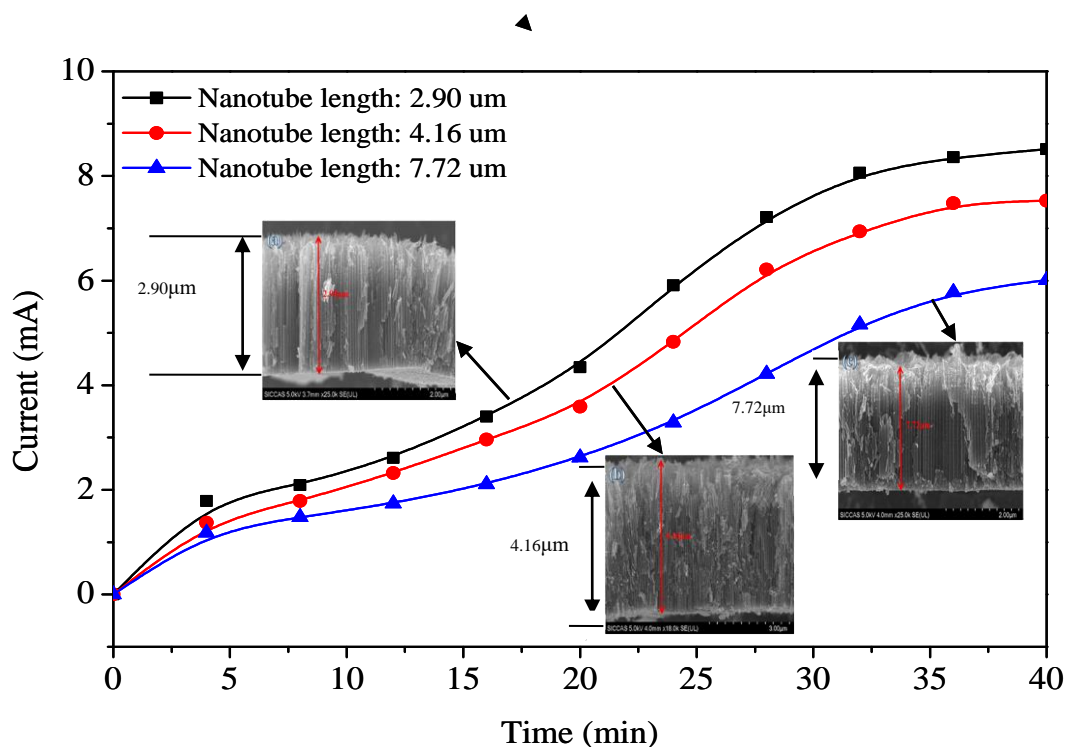


Figure 4. Photocurrent response of TNTs with different nanotube length during PEC process.

The more excellent PEC activity for shorter TNTs length may due to two reasons: firstly, shorter TNTs length means less electric resistance on directed-moving photo-generated charges during PEC process, hence generating higher photo-current and better PEC activity; secondary, fabrication of TNTs is essentially an electrochemical corrosion process, which weakens the junction between TNTs and Ti substrate. Consequently, the shorter the anodization time, the less the corrosion and the stronger adhesion between TNTs and Ti substrate, which means less electric resistance on the junction.

3.3 Influence of integrity of anodic TiO_2 nanotubes on MO degradation activity

The impact of the integrity of annealed TNTs on its PEC was investigated, and the results are presented in Figure 5. In order to create different degree of integrity, annealing with different time is performed. Apparently, TNTs with extending annealing time presents worse integrity and PEC activity. E.g.: It takes 28 min for TNTs with better integrity to reach 98% degradation percentage, which is 4 min less than that for TNTs with worse integrity. In terms of the photocurrent response, that of TNTs with better integrity is apparently higher (annealing time: 1h) than that of worse integrity (annealing time: 3h) (Figure 6). The XRD patterns of annealed TNTs are also researched, and the results are exhibited in Figure 7. The results indicated no essential difference between TNTs with better and worse integrity, which means no difference in crystal form and crystallinity.

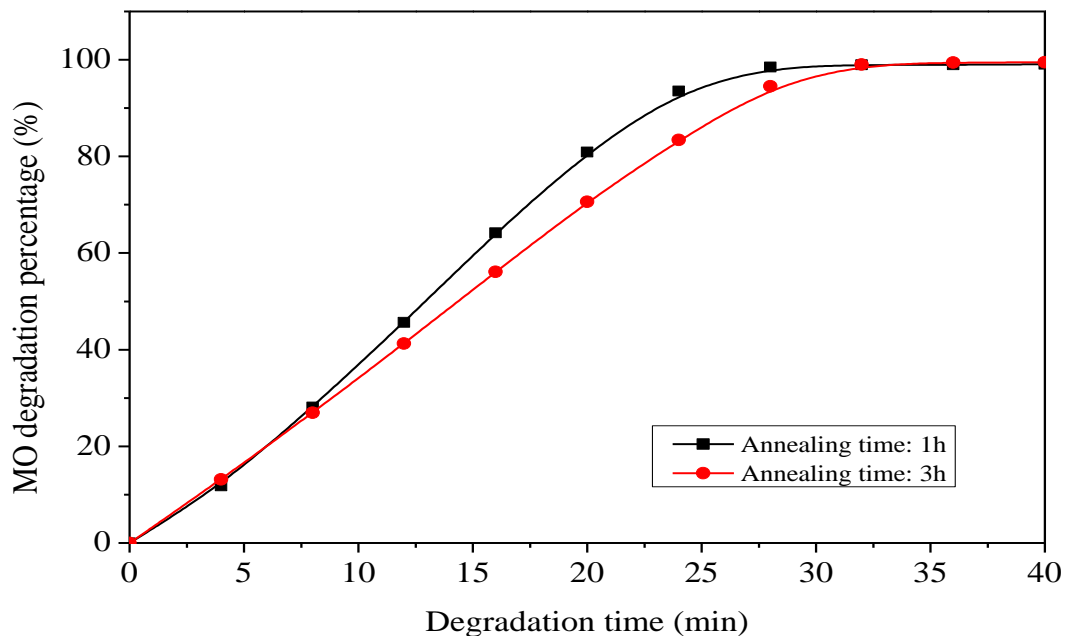


Figure 5. The impacts of the integrity on the PEC activity of anodized TNTs. Here different annealing time generates annealed TNTs with different integrity.

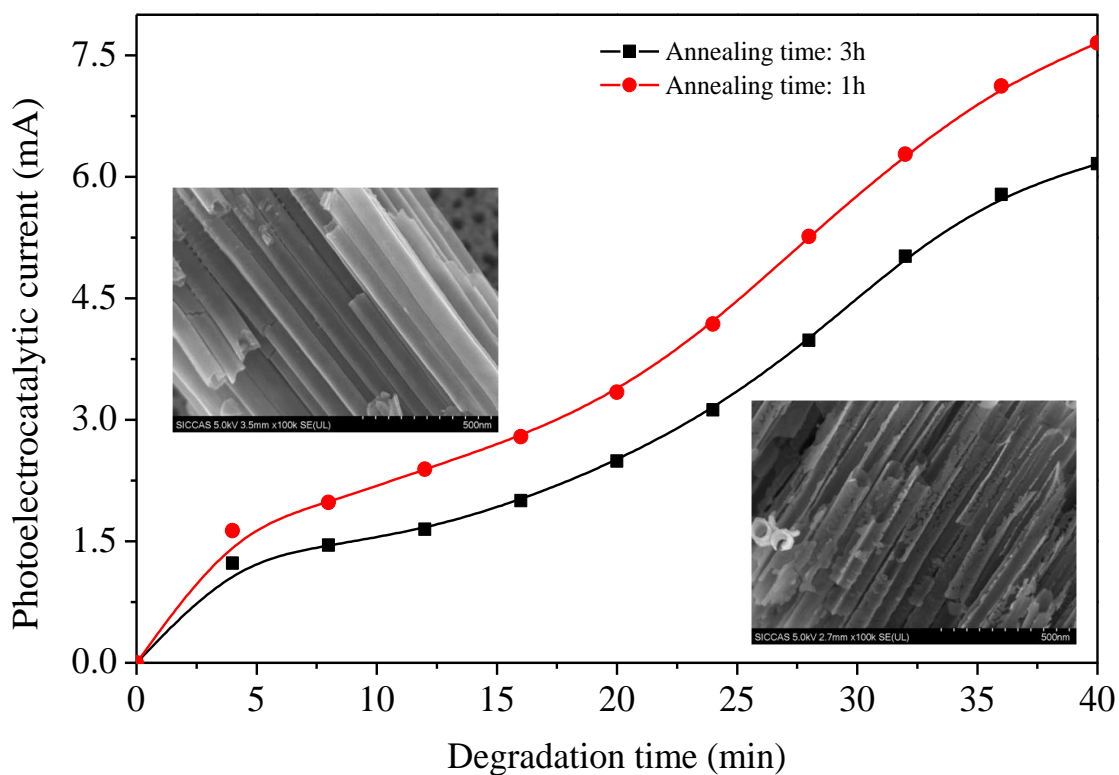


Figure 6. Photocurrent response of TNTs with different integrity during PEC process.

Consequently, the difference in PEC activity between TNTs with better and worse integrity is not related to its crystal form and crystallinity.

Apparently, for TNTs with worse integrity, more cracks and breaks are generated along TiO_2 nanotubes (Figure 6), and it's logical to predict a less junction between TNTs and Ti substrate. During anodization process, strain is generated within TNTs. The subsequent proper annealing may eliminate most of the strain, while severe annealing may release the strain, and cause cracks and breaks, the more the annealing time, the more cracks and breaks generated. Consequently, the directional moving of photo-generated charger will be hindered by the existence of cracks and breaks, and presents lower photo-current and worse PEC activity.

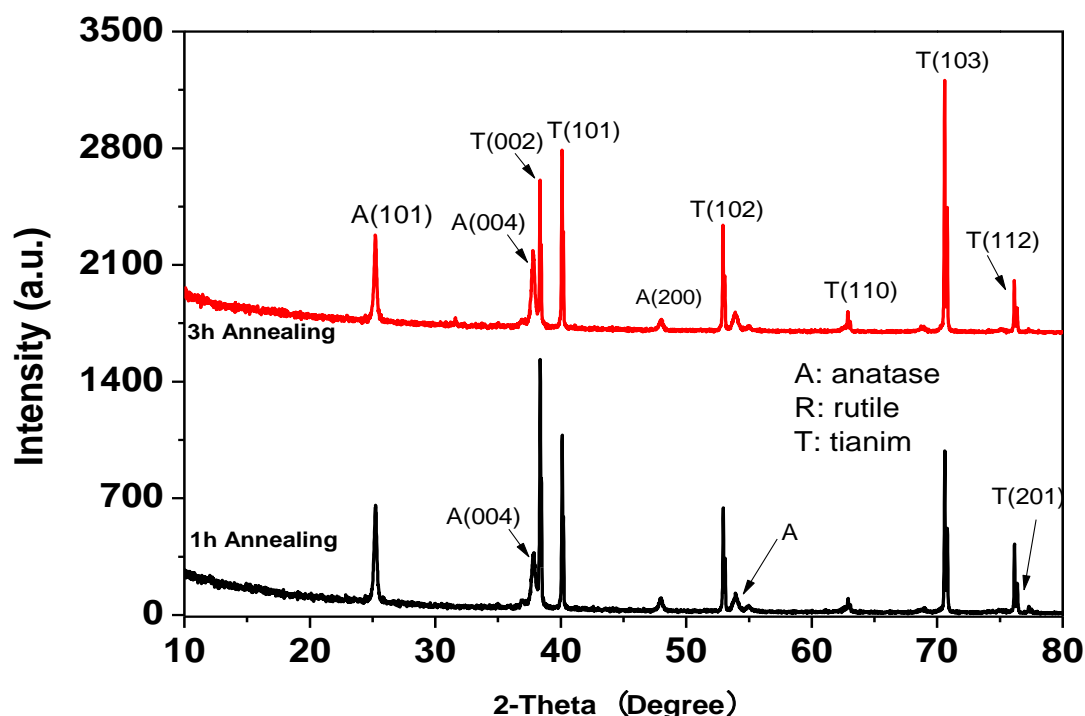


Figure 7. The XRD patterns of anodized TNTs with different annealing time.

3.4 Effects of crystallographic orientation of TiO_2 nanotubes towards MO degradation

The impact of crystallographic orientation of TNTs on its PEC was investigated, and the results are presented in Figure 8. In order to fabricate TNTs with different crystallographic orientation, electrolyte with different water content is applied [36]. Accordingly, PEC activity of prefer-oriented TNTs (P-TNTs) is much better than that of randomly-oriented TNTs (R-TNTs). E.g.: It takes 24 min for P-TNTs to reach 98% degradation percentage, which is 16 min less than that for R-TNTs (Figure 8). The XRD patterns of annealed TNTs with different crystallographic orientation are also researched, and the results are exhibited in Figure 9. The peak intensity of both anatase type P-TNTs and R-TNTs show no significant difference except at $2\theta=37.8$, in which the peak intensity of anatase type P-TNTs is much higher than that of R-TNTs. Apparently, TNTs with 2 % water contents (P-TNTs) presents better crystallographic orientation than that of 5% water contents (R-TNTs) .

In terms of the photocurrent response, that of TNTs with better integrity is apparently higher (P-TNTs) than that of worse integrity (R-TNTs) (Figure 10). Cross-sectional views of TNTs are also

displayed in Figure 10. The average nanotube pore diameters of P-TNTs and R-TNTs are 97.2 and 94.3 nm with wall thicknesses of 12.9 and 11.9 nm, respectively. The nanotube lengths are estimated as 3.6 and 4.16 μm , respectively. The dimensional difference between P-TNTs and R-TNTs is actually indistinctive if the measurement error is considered. Consequently, the difference in PEC activity between P-TNTs and R-TNTs is mainly due to the crystallographic orientation.

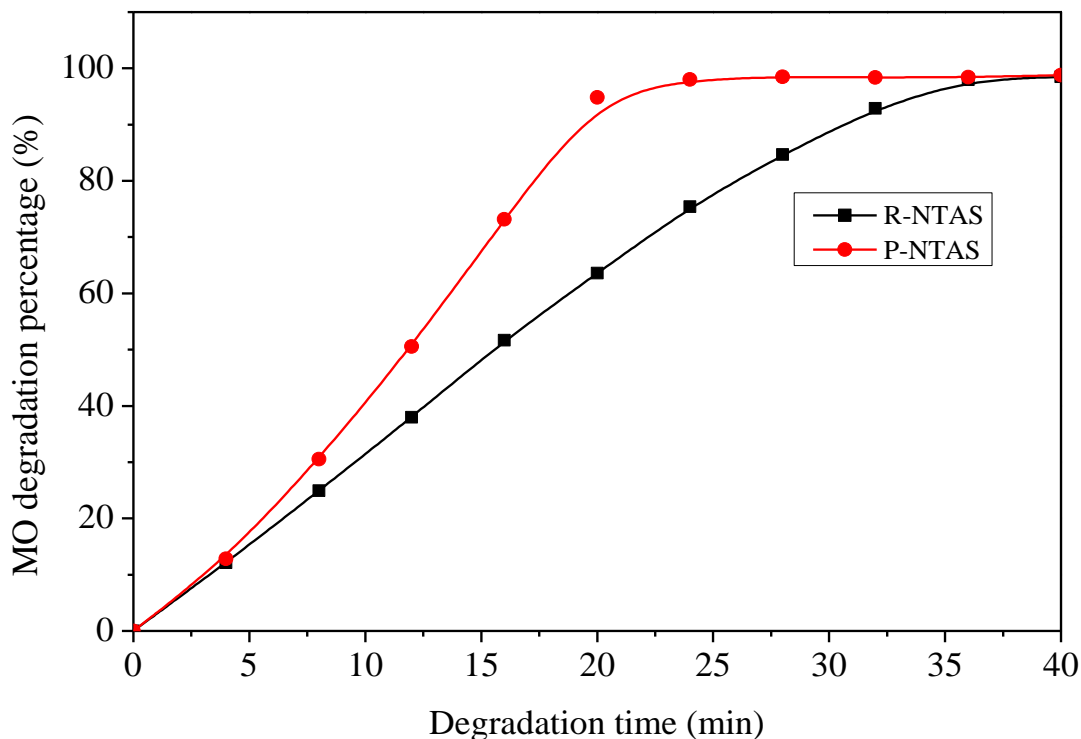


Figure 8. The impacts of crystallographic orientation of TNTs on its PEC activity. Here TNTs with different crystallographic orientation was prepared by anodization of Ti foil in electrolyte with different water content (2 & 5% VOL).

Lee et al. revealed that the P-TNTs showed a preferred orientation along the [001] direction of the anatase crystal structure, and faster electron transport, which is supported by the photocurrent results [36]. Consequently, the directional moving of photo-generated charger will be accelerated due to the preferred orientation of rutile crystal within P-TNTs, and accordingly improve its PEC activity.

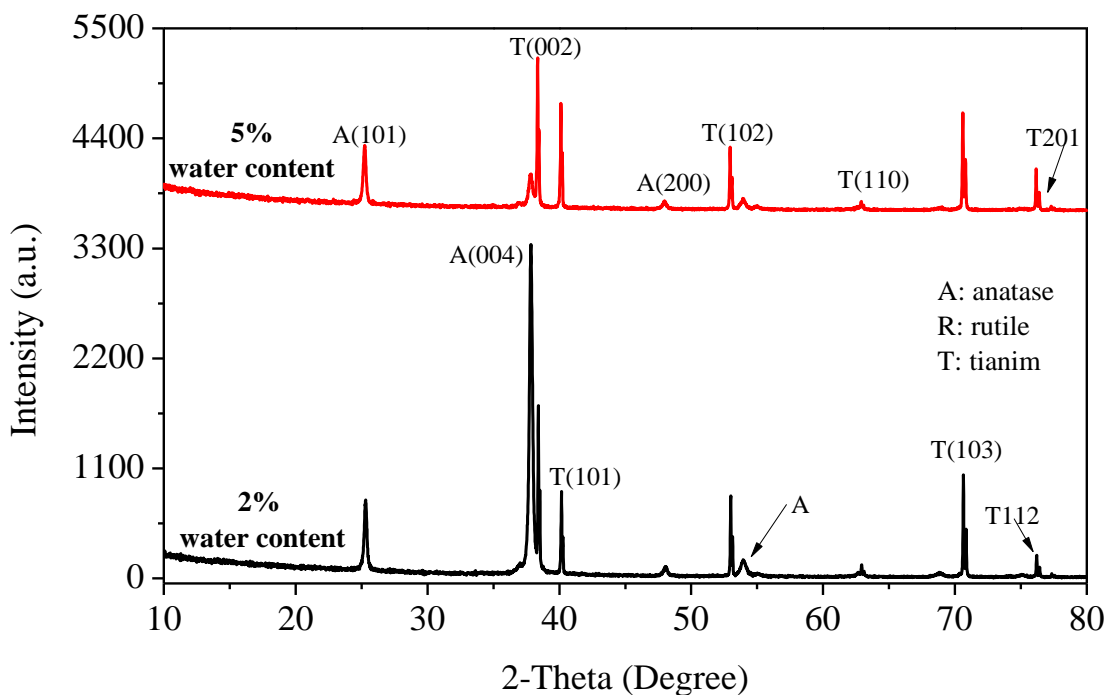


Figure 9. XRD patterns of TNTs with different crystallographic orientation. here 2% water content yields prefer oriented TNTs, and 5% water content yields radom oriented TNTs.

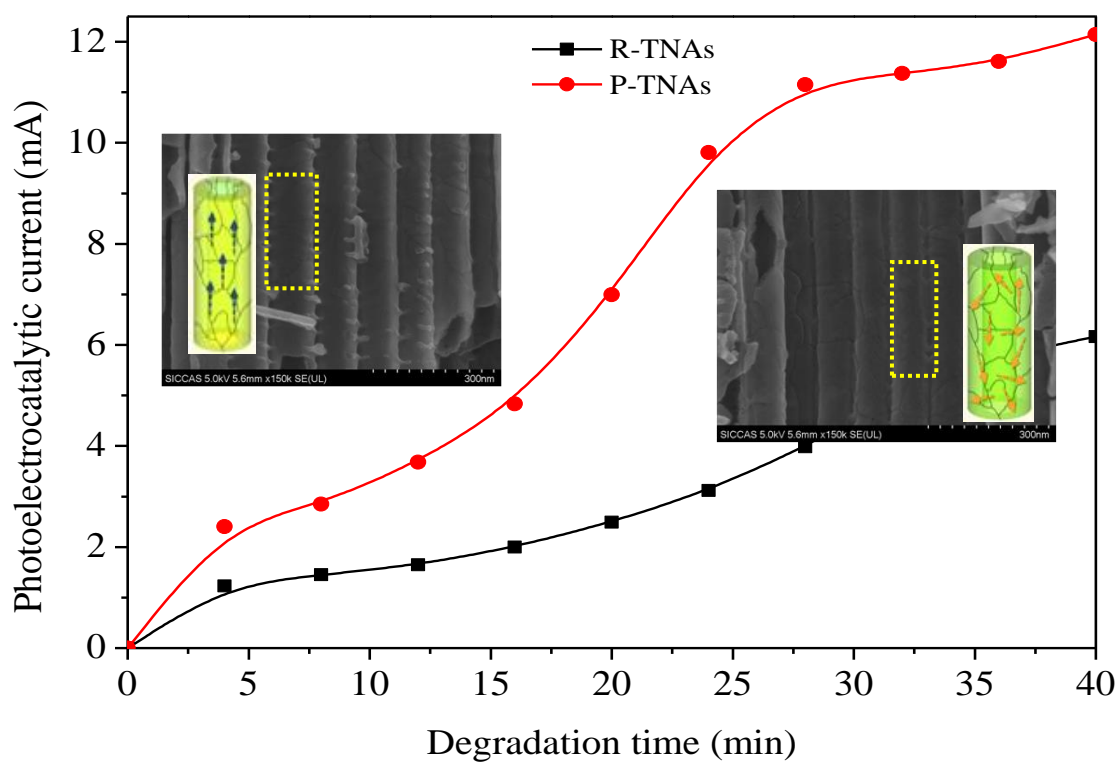


Figure 10. Photocurrent response of TNTs with different crystallographic orientation during PEC process.

4. CONCLUSIONS

Here, the influence of TNTs structure on its PEC activity is explored systematically. The PEC activity of TNTs increases with its length. It only takes 28 min for 2.90 μm long TNTs to reach 98% degradation percentage, in comparison with that of 40 min for 7.72 μm long TNTs. Better integrity and smoothness of TNTs presents better PEC activity. E.g.: TNTs annealed at 350 °C for 1h presents better integrity and only take 28 min to obtain 98% degradation percentage, in comparison with that of 32 min for TNTs annealed at 350 °C for 3h. The crystal structure of P-TNTs shows better PEC activity than that of R-TNTs. E.g.: it only takes 24 min for P-TNTs to reach 98% degradation percentage, in comparison with that of 36 min for R-TNTs. Consequently, it's quite important to optimize the structure of TNTs in order to achieve excellent PEC activity.

ACKNOWLEDGEMENTS

This work was funded by Shanghai Committee of Science and Technology (No.16ZR1414800), Shanghai International Fund for scientific and technological cooperation (No.17230732300), Shanghai International Cooperation Fund Project (No. 17230732300) and Technology Innovation and Energy Level Promotion Project of Shanghai SASASA (No. 2018001). The authors would like to thank the college of Marine Science and Engineering for providing access to their laboratory.

References

1. C. Ampelli, G. Centi, R. Passalacqua, and S. Perathoner, *Energ. Environ. Sci.*, 3 (2010) 292.
2. G. K. Mor, K. Shankar, M. Paulose, O. K. Varghese, and C. A. Grimes, *Nano Lett.*, 6 (2006) 215.
3. B. Tian *et al.*, *nature*, 449 (2007) 885.
4. Z. Zhang and P. Wang, *Energ. Environ. Sci.*, 5 (2012) 6506.
5. S. Garcia-Segura and E. Brillas, *J. Photoch. Photobio C*, 31 (2017) 1.
6. X. Zhou, Y. Zheng, D. Liu, and S. Zhou, *Int. J. Photoenergy*, 2014 (2014) 1.
7. Q. Zhang, J. Zhu, Y. Wang, J. Feng, W. Yan, and H. Xu, *App. Surf. Sci.*, 308 (2014) 161.
8. J. Wu, H. Xu, and W. Yan, *App. Surf. Sci.*, 386 (2016) 1.
9. B. Ayoubi-Feiz, M. H. Mashhadizadeh, and M. Sheydaei, *Sep. Purif. Technol.*, 211 (2019) 704.
10. Y. Hunge, A. Yadav, M. Mahadik, V. Mathe, and C. Bhosale, *J. Taiwan Inst. Chem. E.*, 85 (2018) 273.
11. D. Li, J. Jia, Y. Zhang, N. Wang, X. Guo, and X. Yu, *J. hazard. mater.*, 315 (2016) 1.
12. W. Choi, J. Y. Ko, H. Park, and J. S. Chung, *Appl. Catal. B: Environ.*, 31 (2001) 209.
13. H. Einaga, S. Futamura, and T. Ibusuki, *Appl. Catal. B: Environ.*, 38 (2002) 215.
14. J. M. Macak, M. Zlamal, J. Krysa, and P. Schmuki, *small*, 3 (2007) 300.
15. W. Leng, Z. Zhang, J. Zhang, and C. Cao, *J. Phys. Chem. B*, 109 (2005) 15008.
16. R. Beranek *et al.*, *Appl. Phys. Lett.*, 87 (2005) 37.
17. X. Cheng, Q. Cheng, X. Deng, P. Wang, and H. Liu, *Chemosphere*, 144 (2016) 888.
18. D. Gong *et al.*, *J. Mater. Res.*, 16 (2001) 3331.
19. K. Raja, T. Gandhi, and M. Misra, *Electrochem. Commun.*, 9 (2007) 1069.
20. A. Fujishima, T. N. Rao, and D. A. Tryk, *J. Photoch. Photobio. C*, 1 (2000) 1.
21. J. M. Macák, H. Tsuchiya, and P. Schmuki, *Angew. Chem. Int. Edit.*, 44 (2005) 2100.
22. J. M. Macak, H. Tsuchiya, L. Taveira, S. Aldabergerova, and P. Schmuki, *Angew. Chem. Int. Edit.*, 44 (2005) 7463.
23. K. Shankar, G. K. Mor, A. Fitzgerald, and C. A. Grimes, *J. Phys. Chem. C*, 111 (2007) 21.

24. H. Liu *et al.*, *Chemosphere*, 93 (2013) 160.
25. X. Quan, X. Ruan, H. Zhao, S. Chen, and Y. Zhao, *Environ. Pollut.*, 147 (2007) 409.
26. V. Mohite *et al.*, *Ceram.Int.*, 41 (2015) 2202.
27. V. Mohite *et al.*, *J. Photoch.Photobio. B*, 142 (2015) 204.
28. L. Lei, Y. Su, M. Zhou, X. Zhang, and X. Chen, *Mater. Res. Bull.*, 142 (2007) 2230.
29. J. Díaz-Real, G. Dubed-Bandomo, J. Galindo-De-La-Rosa, E. Ortiz-Ortega, J. Ledesma-García, and L. Arriaga, *Appl. Catal. B-Environ.*, 222 (2018) 18.
30. G. Li, X. Liu, T. An, H. Yang, S. Zhang, and H. Zhao, *Catal.Today*, 242 (2015) 363.
31. M.-Z. Ge *et al.*, *Nanotechnol. Rev.*, 5 (2016) 75.
32. Z. Liu *et al.*, *J. Phys. Chem. C*, 112 (2008) 253.
33. R. Li, S. E. Williams, Q. Li, J. Zhang, C. Yang, and A. Zhou, *Electrocatalysis-US*, 5 (2014) 379.
34. Z. Zhang *et al.*, *Environ. Sci. Technol.*, 41 (2007) 6259.
35. R. J. Candal, W. A. Zeltner, and M. A. Anderson, *Environ. Sci. Technol.*, 34 (2000) 3443.
36. S. Lee *et al.*, *Energ. Environ. Sci.*, 5 (2012) 7989.

© 2020 The Authors. Published by ESG (www.electrochemsci.org). This article is an open access article distributed under the terms and conditions of the Creative Commons Attribution license (<http://creativecommons.org/licenses/by/4.0/>).